SEMM REPORT
UCB/SEMM-90/07

STRUCTURAL ENGINEERING,
MECHANICS AND MATERIALS

# FINITE ELEMENT FORMULATIONS OF INCOMPRESSIBLE RUBBERLIKE MEMBRANE SHELLS

by

F. Gruttmann and R.L. Taylor

JUNE 1990

DEPARTMENT OF CIVIL ENGINEERING
UNIVERSITY OF CALIFORNIA
BERKELEY, CALIFORNIA

# FINITE ELEMENT FORMULATIONS OF INCOMPRESSIBLE RUBBERLIKE MEMBRANE SHELLS

**F. Gruttmann and R.L. Taylor**
Department of Civil Engineering
University of California, Berkeley

## 1. Introduction

The subject of this paper is the nonlinear analysis of thin walled membrane shells with arbitrary geometry. Many applications in engineering and biomechanics are structures which are subjected to large displacements and large strains. These problems (e.g., the inflation of a rubber balloon) are characterized by a nonlinear behavior. Thus, the formulation has both geometrical and material nonlinearity. Constitutive models for finite elasticity written in terms of principal stretches are very useful to model rubberlike materials (e.g., see Treloar [11] and Ogden [5]). The strain energy function of Ogden [5] describes a broad class of incompressible isotropic elastic materials with finite strains. This representation includes as special cases the well known Neo-Hookean and Mooney-Rivlin materials.

For plane strain, axisymmetric, and three dimensional applications a finite element formulation is given by Simo and Taylor [10]. A closed-form expression for the tangent moduli is presented and the numerical solutions are based on a three-field variational principle.

Needleman [4] studies the inflation of spherical rubber balloons used in meteorological applications. The axisymmetric equilibrium is determined numerically within a Ritz-Galerkin method. Wriggers and Taylor [12] present a finite element formulation for this class of problems using a simple conical axisymmetric membrane element.

Our formulation for general shaped membranes requires the computation and linearization of the principle stretches. The principle stretches are eigenvalues of the right stretch tensor **U**, which is defined by the polar decomposition of the material deformation gradient.

First we discuss the kinematics of thin membranes with arbitrary shape. The eigenvalues of the membrane strains are derived using an orthogonal transformation. This computation may be achieved in the tangential plane associated with a point on the membrane surface. Thus the transformation can be written as a function of one plane rotation angle. Singularities, which occur with this approach, are avoided by a small pertubation within the numerical process. Furthermore, the linearization of the principal stretches is presented in a closed form.

The constitutive model is written in terms of the principal values of the right stretch tensor. We are able to satisfy incompressibility in an exact manner using the plane stress condition. For isotropic material response the contravariant components of the Second Piola-Kirchhoff stress tensor are recovered by an orthogonal transformation of the principal stresses. We also derive the linearization of the stress vector as a function of the work conjugate strains.

The variational formulation of equilibrium is formulated in a material description. We consider displacement dependent pressure loads acting normal to the deformed membrane surface. Thus the linearization of the weak form of equilibrium yields an unsymmetric tangent matrix.

A finite element formulation of the membrane theory is presented. The aim of the numerical formulation is to obtain a robust finite element implementation which allows large load steps. We construct isoparametric four and nine node elements based on the displacement method. Several numerical examples are presented that illustrate the effectiveness of the proposed formulation.

## 2. Surface Geometry of an Arbitrary Curved Membrane Shell

In this section the kinematics of thin membrane shells are described. The membrane is assumed to be a smooth, continuous, and differiantiable surface. The thickness $h_0$ of the initial configuration, denoted as $\Omega_0$, is small compared to the smallest radius of curvature. Material points of the membrane surface are labeled with convective coordinates $(\xi, \eta)$. In the definitions and relations that follow Greek superscripts and subscripts refer to contravariant and covariant surface tensor components, respectively. The summation convention applies to each repeated pair of contravariant and covariant indices. Commas are used to denote partial differentiation based on the geometry of the undeformed membrane.

The position vectors $\mathbf{x}(\xi,\eta) = x_i\,\mathbf{e}_i$ and $\mathbf{X}(\xi,\eta) = X_i\,\mathbf{e}_i$ of the current and initial configuration, respectively, are related through the expression $\mathbf{x} = \mathbf{X} + \mathbf{u}$. Here, $\mathbf{u} = u_i\,\mathbf{e}_i$ denotes the displacement vector with respect to the fixed cartesian basis $\mathbf{e}_i$. Then the membrane strain tensor $E_{\alpha\beta}$ is defined by (e.g., see Budianski [1])

$$E_{\alpha\beta} = \frac{1}{2}(g_{\alpha\beta} - G_{\alpha\beta}) \tag{2.1}$$

where the metric coefficients of the deformed and undeformed membrane are given with

$$g_{\alpha\beta} = \mathbf{x}_{,\alpha}\cdot\mathbf{x}_{,\beta} \quad , \quad G_{\alpha\beta} = \mathbf{X}_{,\alpha}\cdot\mathbf{X}_{,\beta}\ . \tag{2.2}$$

With $(2.2)_1$ the principal stretches $\lambda_1$ and $\lambda_2$ of the right stretch tensor $\mathbf{U}$ are determined. These quantities are used in section 3 to compute the stresses. Since $\mathbf{U}$ may be obtained with the symmetric right Cauchy-Green tensor $\mathbf{C} = \mathbf{U}^2$, the principal values $\lambda_\alpha$ follow from the orthogonal transformation

$$\mathbf{C} = \mathbf{R}\hat{\mathbf{C}}\mathbf{R}^{\mathbf{T}}\,. \tag{2.3}$$

Within a matrix notation the following matrices are used

$$\mathbf{C} = \begin{bmatrix} g_{11} & g_{12} \\ g_{21} & g_{22} \end{bmatrix} \quad , \quad \mathbf{R} = \begin{bmatrix} \cos\varphi & -\sin\varphi \\ \sin\varphi & \cos\varphi \end{bmatrix} \quad , \quad \widehat{\mathbf{C}} = \begin{bmatrix} \lambda_1^2 & 0 \\ 0 & \lambda_2^2 \end{bmatrix} . \tag{2.4}$$

Inversion of (2.3) yields the vector of the principle stretches

$$\mathbf{\Lambda} = \widehat{\mathbf{R}}\,\mathbf{G}, \tag{2.5}$$

where

$$\mathbf{\Lambda} = \begin{bmatrix} \widehat{C}_{11} \\ \widehat{C}_{22} \\ 2\widehat{C}_{12} \end{bmatrix} = \begin{bmatrix} \lambda_1^2 \\ \lambda_2^2 \\ 0 \end{bmatrix} \quad , \quad \mathbf{G} = \begin{bmatrix} g_{11} \\ g_{22} \\ 2g_{12} \end{bmatrix} ,$$

$$\widehat{\mathbf{R}} = \begin{bmatrix} \cos^2\varphi & \sin^2\varphi & \sin\varphi\cos\varphi \\ \sin^2\varphi & \cos^2\varphi & -\sin\varphi\cos\varphi \\ -2\sin\varphi\cos\varphi & 2\sin\varphi\cos\varphi & \cos^2\varphi - \sin^2\varphi \end{bmatrix} . \tag{2.6}$$

Using the constraint

$$\widehat{C}_{12} = \widehat{C}_{21} = -\frac{1}{2}(g_{11} - g_{22})\,\sin 2\varphi + g_{12}\,\cos 2\varphi \equiv 0 \tag{2.7}$$

we get the angle $\varphi$

$$\varphi = \frac{1}{2}\arctan\frac{2g_{12}}{g_{11} - g_{22}} . \tag{2.8}$$

The denominator in (2.8) may take the value zero, however in the numerical process this singularity can be avoided by a small pertubation.

Incompressibility is expressed by the identity $J = det\,\mathbf{F} = \lambda_1\,\lambda_2\,\lambda_3 \equiv 1$ where $\mathbf{F}$ is the material deformation gradient. Thus the principle stretch $\lambda_3$, normal to the membrane, is given

$$\lambda_3 = (\lambda_1\lambda_2)^{-1} . \tag{2.9}$$

Furthermore, we are able to compute the current thickness of the membrane $h = h_0(\lambda_1\lambda_2)^{-1}$ as a function of the principle stretches and the initial thickness $h_0$.

In the last part of this section we present the derivatives of $\lambda_\alpha$ with respect to $E_{\alpha\beta}$

$$\begin{bmatrix} \frac{\partial \widehat{C}_{11}}{\partial g_{11}} & \frac{\partial \widehat{C}_{11}}{\partial g_{22}} & \frac{\partial \widehat{C}_{11}}{\partial (2g_{12})} \\ \frac{\partial \widehat{C}_{22}}{\partial g_{11}} & \frac{\partial \widehat{C}_{22}}{\partial g_{22}} & \frac{\partial \widehat{C}_{22}}{\partial (2g_{12})} \\ \frac{\partial (2\widehat{C}_{12})}{\partial g_{11}} & \frac{\partial (2\widehat{C}_{12})}{\partial g_{22}} & \frac{\partial (2\widehat{C}_{12})}{\partial (2g_{12})} \end{bmatrix} = \begin{bmatrix} \lambda_1 \frac{\partial \lambda_1}{\partial E_{11}} & \lambda_1 \frac{\partial \lambda_1}{\partial E_{22}} & \lambda_1 \frac{\partial \lambda_1}{\partial (2E_{12})} \\ \lambda_2 \frac{\partial \lambda_2}{\partial E_{11}} & \lambda_2 \frac{\partial \lambda_2}{\partial E_{22}} & \lambda_2 \frac{\partial \lambda_2}{\partial (2E_{12})} \\ \frac{\partial (2\widehat{C}_{12})}{\partial E_{11}} & \frac{\partial (2\widehat{C}_{12})}{\partial E_{22}} & \frac{\partial (2\widehat{C}_{12})}{\partial (2E_{12})} \end{bmatrix} = \widehat{\mathbf{R}}. \tag{2.10}$$

It should be noted, that the differentiation of $\lambda_\alpha^2$ with respect to $\varphi$ yields the identity (2.7) and therefore vanishes. Furthermore we compute the derivative of $\widehat{C}_{12}$ with respect to $E_{\alpha\beta}$

$$\frac{\partial \widehat{C}_{12}}{\partial E_{\alpha\beta}} + \frac{\partial \widehat{C}_{12}}{\partial \varphi} \frac{\partial \varphi}{\partial E_{\alpha\beta}} = 0. \tag{2.11}$$

With (2.7) and (2.11) the linearization of $\varphi$ follows

$$\begin{bmatrix} \frac{\partial \varphi}{\partial E_{11}} \\ \frac{\partial \varphi}{\partial E_{22}} \\ \frac{\partial \varphi}{\partial (2E_{12})} \end{bmatrix} = -\left(\frac{\partial \widehat{C}_{12}}{\partial \varphi}\right)^{-1} \begin{bmatrix} \frac{\partial \widehat{C}_{12}}{\partial E_{11}} \\ \frac{\partial \widehat{C}_{12}}{\partial E_{22}} \\ \frac{\partial \widehat{C}_{12}}{\partial (2E_{12})} \end{bmatrix} = \frac{\cos 2\varphi}{g_{11} - g_{22}} \begin{bmatrix} -\sin 2\varphi \\ \sin 2\varphi \\ \cos 2\varphi \end{bmatrix}. \tag{2.12}$$

These matrices are used to linearize the constitutive equations in the following section.

Remark:

The principal stretches $\lambda_\alpha$ are the eigenvalues of the right stretch tensor $\mathbf{U}$. Thus it is also possible to accomplish the multiplicative decomposition of the material deformation gradient, which yields a symmetric stretch tensor and a rotation tensor. In this case it is useful to formulate the weak form of the equilibrium in terms of the Biot stress tensor, which is work conjugate to $\mathbf{U}$ (e.g., see Gruttmann [2]). Subsequently, the eigenvalue problem can be solved to recover the stretches $\lambda_\alpha$.

## 3. Constitutive Equations and Linearization

In this section we present constitutive equations for an incompressible rubberlike material. The application of these equations to thin membranes and the linearization of the stress strain relations are also given.

### 3.1 Computation of the Stresses

For the isotropic incompressible elastic solids considered here, the existence of a strain energy function $W$ is postulated. The strain energy is an isotropic function of the principal stretches $\lambda_i$ and Here, $W$ is written as

$$W(\lambda_i) = \sum_r \frac{\mu_r}{\alpha_r}[\lambda_1^{\alpha_r} + \lambda_2^{\alpha_r} + \lambda_3^{\alpha_r} - 3]\,. \tag{3.1}$$

This presentation was first proposed by Ogden [5] where $\mu_r$ and $\alpha_r$ are constants. The summation on $r$ extends over as many terms as are necessary to characterize a particular material. The exponents $\alpha_r$ may take any nonzero real value.

Using the incompressibility constraint (2.9) the strain energy can be expressed as a function of the independent stretches $\lambda_1$ and $\lambda_2$

$$W(\lambda_\gamma) = \sum_r \frac{\mu_r}{\alpha_r}[\lambda_1^{\alpha_r} + \lambda_2^{\alpha_r} + (\lambda_1\lambda_2)^{-\alpha_r} - 3]\,. \tag{3.2}$$

Since we assume hyperelastic material response, the Second Piola-Kirchhoff stress tensor $\mathbf{S}$ follows from differentiation of $W$ with respect to the work conjugate Green Lagrangian strain tensor $\mathbf{E}$. The components of $\mathbf{S}$ are given by the chain rule

$$S^{\alpha\beta} = \frac{\partial W(\lambda_\gamma)}{\partial E_{\alpha\beta}} = \frac{\partial W}{\partial \lambda_1}\frac{\partial \lambda_1}{\partial E_{\alpha\beta}} + \frac{\partial W}{\partial \lambda_2}\frac{\partial \lambda_2}{\partial E_{\alpha\beta}}\,. \tag{3.3}$$

Due to the plane stress assumption the stresses $S^{\alpha 3}$ are vanishing. Using (3.3) we are able to define the principal values $S_\gamma$ of the Second Piola-Kirchhoff stress tensor

$$S_\gamma = \lambda_\gamma^{-1}\frac{\partial W}{\partial \lambda_\gamma} = \lambda_\gamma^{-2}\sum_r \mu_r[\lambda_\gamma^{\alpha_r} - (\lambda_1\lambda_2)^{-\alpha_r}] \qquad (\gamma = 1,2)\,. \tag{3.4}$$

Hence, the principal values of the Cauchy stress tensor $\boldsymbol{\sigma}$ are given by the transformation

$$\sigma_\gamma = \lambda_\gamma^2 S_\gamma = \sum_r \mu_r [\lambda_\gamma^{\alpha_r} - (\lambda_1 \lambda_2)^{-\alpha_r}]. \tag{3.5}$$

The derivatives of the stretches $\lambda_\gamma$ with respect to $E_{\alpha\beta}$ are presented in (2.10). Thus we are able to compute the stresses $S^{\alpha\beta}$

$$\mathbf{S} = \hat{\mathbf{R}}^T \hat{\mathbf{S}}, \tag{3.6}$$

where

$$\mathbf{S} = \begin{bmatrix} S^{11} \\ S^{22} \\ S^{12} \end{bmatrix} \quad , \quad \hat{\mathbf{S}} = \begin{bmatrix} S_1 \\ S_2 \\ 0 \end{bmatrix}. \tag{3.7}$$

Remark:

It is also possible to derive equation (3.6) by transformation of the principal stresses

$$\bar{\mathbf{S}} = \mathbf{R} \tilde{\mathbf{S}} \mathbf{R}^T, \tag{3.8}$$

where

$$\bar{\mathbf{S}} = \begin{bmatrix} S^{11} & S^{12} \\ S^{21} & S^{22} \end{bmatrix} \quad , \quad \mathbf{R} = \begin{bmatrix} \cos\varphi & -\sin\varphi \\ \sin\varphi & \cos\varphi \end{bmatrix} \quad , \quad \tilde{\mathbf{S}} = \begin{bmatrix} S_1 & 0 \\ 0 & S_2 \end{bmatrix}. \tag{3.9}$$

Substituting (3.9) into (3.8) we obtain the transformed stresses (3.6). For isotropic material response the rotation angle $\varphi$ is given by (2.8), since $\mathbf{C}$ and $\bar{\mathbf{S}}$ have the same eigenvectors.

## 3.2 Linearization of the Second Piola-Kirchhoff Stresses

In this section the linearization of the stresses defined by (3.6) is derived. Therefore we need to determine the derivatives of $S^{\alpha\beta}$ with respect to the work conjugate strains $E_{\alpha\beta}$. Using (2.10), (2.12), and (3.5) the linearization of $S_\alpha$ and $\varphi$ yields the symmetric material tangent matrix

$$\mathbf{C}_T = \hat{\mathbf{R}}^T \bar{\mathbf{C}} \hat{\mathbf{R}} = \begin{bmatrix} \frac{\partial S^{11}}{\partial E_{11}} & \frac{\partial S^{11}}{\partial E_{22}} & \frac{\partial S^{11}}{\partial (2E_{12})} \\ \frac{\partial S^{22}}{\partial E_{11}} & \frac{\partial S^{22}}{\partial E_{22}} & \frac{\partial S^{22}}{\partial (2E_{12})} \\ \frac{\partial S^{12}}{\partial E_{11}} & \frac{\partial S^{12}}{\partial E_{22}} & \frac{\partial S^{12}}{\partial (2E_{12})} \end{bmatrix}, \tag{3.10}$$

where

$$\bar{\mathbf{C}} = \begin{bmatrix} \frac{1}{\lambda_1}\frac{\partial S_1}{\partial \lambda_1} & \frac{1}{\lambda_2}\frac{\partial S_1}{\partial \lambda_2} & 0 \\ \frac{1}{\lambda_1}\frac{\partial S_2}{\partial \lambda_1} & \frac{1}{\lambda_2}\frac{\partial S_2}{\partial \lambda_2} & 0 \\ 0 & 0 & -(S_1 - S_2)(\frac{\partial \widehat{C}_{12}}{\partial \varphi})^{-1} \end{bmatrix}$$

$$= \begin{bmatrix} \lambda_1^{-4}(\lambda_1 \frac{\partial \sigma_1}{\partial \lambda_1} - 2\sigma_1) & \lambda_1^{-2}\lambda_2^{-2}(\lambda_2 \frac{\partial \sigma_1}{\partial \lambda_2}) & 0 \\ \lambda_1^{-2}\lambda_2^{-2}(\lambda_1 \frac{\partial \sigma_2}{\partial \lambda_1}) & \lambda_2^{-4}(\lambda_2 \frac{\partial \sigma_2}{\partial \lambda_2} - 2\sigma_2) & 0 \\ 0 & 0 & \frac{(S_1 - S_2)\cos 2\varphi}{g_{11} - g_{22}} \end{bmatrix}. \tag{3.11}$$

The derivatives of the Cauchy stresses $\sigma_\alpha$ follow from (3.5)

$$\begin{aligned} \lambda_1 \frac{\partial \sigma_1}{\partial \lambda_1} &= \sum_r \mu_r \alpha_r [\lambda_1^{\alpha_r} + (\lambda_1 \lambda_2)^{-\alpha_r}] \\ \lambda_2 \frac{\partial \sigma_2}{\partial \lambda_2} &= \sum_r \mu_r \alpha_r [\lambda_2^{\alpha_r} + (\lambda_1 \lambda_2)^{-\alpha_r}] \\ \lambda_2 \frac{\partial \sigma_1}{\partial \lambda_2} &= \lambda_1 \frac{\partial \sigma_2}{\partial \lambda_1} = \sum_r \mu_r \alpha_r (\lambda_1 \lambda_2)^{-\alpha_r}. \end{aligned} \tag{3.12}$$

Finally we derive the stiffness $C_T$ for infinitesimal small deformations. The material parameters $\mu_r$ and $\alpha_r$ must fulfil

$$\sum_r \mu_r \alpha_r = 2\mu, \tag{3.13}$$

where $\mu$ is the shear modulus. The component $\bar{C}_{33}(\lambda_\alpha = 1)$ yields an undetermined expression ($\bar{C}_{33}(\lambda_\alpha = 1) = \frac{0}{0}$), however it is possible to derive the limit value

$$\lim_{\lambda_\alpha \to 1} \frac{(S_1 - S_2)\cos 2\varphi}{g_{11} - g_{22}} = \mu. \tag{3.14}$$

Using (3.13) and (3.14) the tangential matrix $C_T$ yields classical Hooke's law for incompressible material behavior

$$\mathbf{C}_T(\lambda_\alpha = 1) = 2\mu \begin{bmatrix} 2 & 1 & 0 \\ 1 & 2 & 0 \\ 0 & 0 & \frac{1}{2} \end{bmatrix} = \frac{E}{1-\nu^2} \begin{bmatrix} 1 & \nu & 0 \\ \nu & 1 & 0 \\ 0 & 0 & \frac{1-\nu}{2} \end{bmatrix}_{\nu=0.5}. \tag{3.15}$$

Here, $E = 2\mu(1+\nu)$ and $\nu$ are Young's modudus and Poisson ratio, respectively. Above equations are used in section 5 to derive the tangent stiffness matrix for the finite element formulation.

## 4. Variational Equation of Equilibrium

External loading is assumed on the membrane surface. We consider a pressure $\mathbf{p}(\mathbf{x}) = p\,\mathbf{n}$ per unit deformed area, acting in the direction of the normal vector $\mathbf{n}$ to the deformed membrane $\Omega$. In this case the principle of virtual work, written for the deformed configuration, is given by (e.g., see Budianski [1])

$$\int_{(\Omega_0)} \mathbf{S} \cdot \delta\mathbf{E}\, h_0\, d\Omega_0 = \int_{(\Omega)} p\,\mathbf{n} \cdot \delta\mathbf{x}\, d\Omega\,. \tag{4.1}$$

The virtual membrane strains $\delta E_{\alpha\beta}$ follow from (2.1) and (2.2)

$$\delta E_{\alpha\beta} = \frac{1}{2}\,(\delta\mathbf{u}_{,\alpha} \cdot \mathbf{x}_{,\beta} + \mathbf{x}_{,\alpha} \cdot \delta\mathbf{u}_{,\beta}\,) \tag{4.2}$$

Furthermore, the unit vector $\mathbf{n}$, which is perpendicular to the deformed membrane, is obtained by the cross product of the tangential vectors $\mathbf{x}_{,\alpha}$

$$\mathbf{n} = \frac{\mathbf{x}_{,1} \times \mathbf{x}_{,2}}{\|\mathbf{x}_{,1} \times \mathbf{x}_{,2}\|}\,. \tag{4.3}$$

Hence, we can transform the current area element $d\Omega$ to the reference configuration as

$$d\Omega = \frac{\|\mathbf{x}_{,1} \times \mathbf{x}_{,2}\|}{\|\mathbf{X}_{,1} \times \mathbf{X}_{,2}\|} d\Omega_0\,. \tag{4.4}$$

Using (4.3) and (4.4), the principle of virtual work becomes

$$g(\mathbf{u}, \delta\mathbf{u}) = \int_{(\Omega_0)} [\mathbf{S} \cdot \delta\mathbf{E}\, h_0 - \frac{p}{\|\mathbf{X}_{,1} \times \mathbf{X}_{,2}\|} (\mathbf{x}_{,1} \times \mathbf{x}_{,2}\,) \cdot \delta\mathbf{u}] d\Omega_0 = 0\,. \tag{4.5}$$

A linearization procedure (e.g., see Hughes and Pister [3]) yields the expression

$$\begin{aligned} Dg(\mathbf{u}, \delta\mathbf{u}) \cdot \Delta\mathbf{u} = \int_{(\Omega_0)} & [(\Delta\mathbf{S} \cdot \delta\mathbf{E} + \mathbf{S} \cdot \Delta\delta\mathbf{E}\,)\, h_0 \\ & - \frac{p}{\|\mathbf{X}_{,1} \times \mathbf{X}_{,2}\|} (\Delta\mathbf{u}_{,1} \times \mathbf{x}_{,2} + \mathbf{x}_{,1} \times \Delta\mathbf{u}_{,2}\,) \cdot \delta\mathbf{u}]\, d\Omega_0 = 0\,. \end{aligned} \tag{4.6}$$

The linearized stresses $\Delta \mathbf{S}$ are presented in section 3 and the incremental virtual strains follow from

$$\Delta\delta E_{\alpha\beta} = \frac{1}{2}\left(\delta\mathbf{u}_{,\alpha}\cdot\Delta\mathbf{u}_{,\beta} + \Delta\mathbf{u}_{,\alpha}\cdot\delta\mathbf{u}_{,\beta}\right). \tag{4.7}$$

For nonconservative loads (4.6) leads to unsymmetric matrices in the finite element formulation (e.g., see Schweizerhof, Ramm [8]).

## 5. Finite Element Formulation

In this section we describe a finite element formulation of the membrane theory presented above. We use a displacement model to construct four to nine node elements. Initial geometry and displacements are approximated using the same shape functions. With this approach we are able to discretize arbitrary curved surfaces.

The following presentation is formulated for a single element, $\Omega_e$. Hence, the position vector of the undeformed membrane and the displacement vector are approximated by the mapping

$$\begin{aligned} \mathbf{X}^h|_{\Omega_e} &= \sum_{I=1}^{n_e} N_I\,\mathbf{X}_I \\ \mathbf{u}^h|_{\Omega_e} &= \sum_{I=1}^{n_e} N_I\,\mathbf{u}_I\,. \end{aligned} \tag{5.1}$$

Here the functions $N_I(\xi,\eta)$ are the isoparametric element shape functions, $n_e$ is the number of nodes per element (4 to 9), and $\mathbf{X}_I, \mathbf{u}_I$, represent the nodal values of $\mathbf{X}^h, \mathbf{u}^h$ within the element $\Omega_e$, respectively. Thus the position vector of the current configuration is given by $\mathbf{x}^h|_{\Omega_e} = \mathbf{X}^h|_{\Omega_e} + \mathbf{u}^h|_{\Omega_e}$.

The finite element approximation of the virtual strains $\delta\boldsymbol{\varepsilon}^h = \{\delta E_{11}, \delta E_{22}, 2\delta E_{12}\}^h$ is written in a matrix notation as

$$\delta\boldsymbol{\varepsilon}^h = \sum_{I=1}^{n_e} \mathbf{B}_I\,\delta\mathbf{u}_I \quad , \quad \mathbf{B}_I = \begin{bmatrix} N_{I,1}\,\mathbf{x}^h{}_{,1}^T \\ N_{I,2}\,\mathbf{x}^h{}_{,2}^T \\ N_{I,1}\,\mathbf{x}^h{}_{,2}^T + N_{I,2}\,\mathbf{x}^h{}_{,1}^T \end{bmatrix}. \tag{5.2}$$

Using the approximation for the displacements (5.1) and for the virtual strains (5.2) we formulate the weak form of the equilibrium (4.5) as

$$g_e(\mathbf{u},\delta\mathbf{u}) = \sum_{I=1}^{n_e} \delta\mathbf{u}_I^T \int_{(\Omega_e)} [\,\mathbf{B}_I^T\,\mathbf{S}^h\,h_0 \;-\; p\,\frac{\mathbf{x}_{,1}^h \times \mathbf{x}_{,2}^h}{\|\mathbf{X}_{,1}^h \times \mathbf{X}_{,2}^h\|}\,N_I\,]\,d\Omega_e = 0\,. \tag{5.3}$$

A vector of stresses $\mathbf{S}^h = \{S^{11}, S^{22}, S^{12}\}^h$ is obtained via the finite element approximation of the material law expressed by (3.3) to (3.7).

To solve the nonlinear equation (5.3) we use a Newton-Raphson procedure. Therefore the finite element approximation of the linearized weak form (4.6)

$$Dg_e(\mathbf{u},\delta\mathbf{u})\Delta\mathbf{u} = \sum_{I=1}^{n_e}\sum_{K=1}^{n_e} \delta\mathbf{u}_I^T\,\mathbf{K}_{IK}\Delta\mathbf{u}_K \tag{5.4}$$

needs to be evaluated for each iteration. In (5.4), $\mathbf{K}_{IK}$ is the tangential stiffness matrix for one node of an element and is deduced from

$$\mathbf{K}_{IK} = \int_{(\Omega_e)} [(\mathbf{B}_I^T\,\mathbf{C}_T\,\mathbf{B}_K \;+\; \mathbf{G}_{IK})\,h_0 \;-\mathbf{P}_{IK}]\,d\Omega_e\,. \tag{5.5}$$

The material matrix $\mathbf{C}_T$ is presented in (3.10) and the geometric matrix $\mathbf{G}_{IK}$ can easily be deduced from (4.7) and expressed as

$$\mathbf{G}_{IK} = \begin{bmatrix} g_{IK} & 0 & 0 \\ 0 & g_{IK} & 0 \\ 0 & 0 & g_{IK} \end{bmatrix} \tag{5.6}$$

where $g_{IK} = S^{11}\,N_{I,1}\,N_{K,1} + S^{22}\,N_{I,2}\,N_{K,2} + S^{12}\,(N_{I,1}\,N_{K,2} + N_{I,2}\,N_{K,1}\,)$. Finally the linearization of the virtual work of the external loads yields the skewsymmetric matrix

$$\mathbf{P}_{IK} = \frac{p}{\|\mathbf{X}^h{}_{,1} \times \mathbf{X}^h{}_{,2}\|} \begin{bmatrix} 0 & -p_{IK}^3 & p_{IK}^2 \\ p_{IK}^3 & 0 & -p_{IK}^1 \\ -p_{IK}^2 & p_{IK}^1 & 0 \end{bmatrix} \tag{5.7}$$

where $p_{IK}^n = (x_{n,1}^h\,N_{I,2} - x_{n,2}^h\,N_{I,1}\,)\,N_K \quad (n = 1,2,3)$.

In the last part of this section we describe the computation of the shape function derivatives $N_{I,\alpha}$. It is useful to introduce an orthonormal basis system $\mathbf{T}_i$ (i=1,2,3)

with associated coordinates $s_i$ in the undeformed configuration of each element. In this case the covariant and contravariant components of the stress and strain tensors are identical. Using the chain rule we obtain the derivatives of the shape functions $\frac{\partial N_I}{\partial s_\alpha} = N_{I,\alpha}$ $(\alpha = 1,2)$

$$\begin{bmatrix} N_{I,1} \\ N_{I,2} \end{bmatrix} = \mathbf{J}^{-1} \begin{bmatrix} N_{I,\xi} \\ N_{I,\eta} \end{bmatrix} \quad , \quad \mathbf{J} = \begin{bmatrix} \frac{\partial s_1}{\partial \xi} & \frac{\partial s_2}{\partial \xi} \\ \frac{\partial s_1}{\partial \eta} & \frac{\partial s_2}{\partial \eta} \end{bmatrix} . \tag{5.8}$$

Thus to complete the process the Jacobian transformation matrix $\mathbf{J}$ needs to be evaluated. We compute the tangential vectors

$$\mathbf{G}_1 = \frac{\partial \mathbf{X}}{\partial \xi} \quad , \quad \mathbf{G}_2 = \frac{\partial \mathbf{X}}{\partial \eta} \tag{5.9}$$

by partial differentiation of the position vector of the undeformed membrane $\mathbf{X}(\xi, \eta)$ with respect to the convective coordinates $\xi$ und $\eta$. The vectors $\mathbf{G}_1$ and $\mathbf{G}_2$ are neither unit vectors nor orthogonal. However, we are able to compute an orthonormal basis system $\mathbf{T}_i$ as follows:

$$\mathbf{T}_n = \frac{\mathbf{G}_1 \times \mathbf{G}_2}{\|\mathbf{G}_1 \times \mathbf{G}_2\|}, \quad \mathbf{T}_1 = \frac{\mathbf{G}_1}{\|\mathbf{G}_1\|}, \quad \mathbf{T}_2 = \mathbf{T}_n \times \mathbf{T}_1 . \tag{5.10}$$

Using (5.9) and (5.10) we express the components of the Jacobian matrix $J_{\alpha\beta} = \mathbf{G}_\alpha \cdot \mathbf{T}_\beta$ $(\alpha, \beta = 1,2)$ (e.g., see Zienkiewicz and Taylor [13]).

Finally the area element $d\Omega_e$ is transformed by the relation

$$d\Omega_e = \| \frac{\partial \mathbf{X}}{\partial \xi} \times \frac{\partial \mathbf{X}}{\partial \eta} \| \, d\xi d\eta \tag{5.11}$$

and substituted into (5.3) and (5.5). The element tangent matrices and the element residual vectors are computed using Gauss quadrature. Each element is assembled to form the global problem using standard procedures.

## 6. Numerical Examples

In this section we present several numerical examples, which demonstrate effectiveness of the finite element formulation presented above. The finite element scheme was implemented using an enhanced version of the program FEAP [13]. All computations were performed using a VAX 8650 computer.

### 6.1 Simple Tension, Equibiaxial Tension and Pure Shear

In the first three examples homogeneous stress states are considered to demonstrate the agreement of our finite element solutions with exact solutions given in the literature. We use the three-term constitutive model of Ogden formulated in principal stretches, as described in section 3. Table 1 summarizes the material constants, chosen by Ogden ([5],[6]) to fit an incompressible rubber material.

**Table 1** Material Properties for an Ogden Model

| r | $\mu_r$ | $\alpha_r$ |
|---|---|---|
| 1 | +6.29947 | +1.3 |
| 2 | +0.01267 | +5.0 |
| 3 | -0.10013 | -2.0 |

These material data give excellent agreement with experimental data on rubber by Treloar [11] for a variety of homogeneous stress states. The following three plane stress states are considered and compared with exact solutions given by Ogden [5]. Figure 1 , 2 and 3 show the results for simple tenson, equibiaxial tension and pure shear, respectively. As shown there is exact agreement between the theoretical solution and our finite element solution. These patch test examples verify the correctness of the finite element implementation.

### 6.2 Inflation of a Spherical Balloon

The inflation of a rubber balloon, loaded by an internal pressure $p$, is considered in the next example. This problem, which shows an instability, is extensively studied in the literature. A closed form theoretical solution for a spherical "balloon" is given by Ogden [6]. Needleman [4] investigates the axisymmetric equilibrium state numerically by means of a Ritz-Galerkin method. A finite element solution with axisymmetric finite elements may be found in the paper of Wriggers and Taylor [12].

We consider a balloon with radius $R = 1$ and thickness $h_0 = .01$ composed of a three-term Ogden model with material constants given in Table 1. Since the stress state is axisymmetric, it is sufficient to approximate a sector of the sphere. We use 20 4-node bilinear isoparametric elements to model a $5^o$ segment of the sphere. To pass the limit point, which occurs in this problem, an arc-length procedure is used in combination with a standard Newton method of solution. The use of the tangential stiffness matrix, derived analyticaly in the previous section, provides a quadratically convergent solution process. Figure 4 shows the plot of the dimensionless pressure $p^*$ against the stretch $\lambda$. According to [4], the dimensionless pressure $p^*$ is defined

$$p^* = \frac{p}{2\,\frac{h_0}{R}\,\sum_r \mu_r \alpha_r}$$

It should be noted that our results agree with those of Ogden [5], Needleman [4] and Wriggers and Taylor [12].

### 6.3 Inflation of a Circular Cylinder

In this example a circular cylinder is loaded by internal pressure (see Wriggers and Taylor [12]). The upper end of the cylinder is fixed in the axial direction and the lower end in the axial and radial directions. The geometrical data are: radius $R = 10$, height $H = 20$ and thickness $h_0 = .1$. The material properties are given in Table 1. Since

the problem is axisymmetric, we use a $1 \times 20$-mesh of 4-node elements to model a $5^0$ sector of the cylinder.

In Figure 5 the internal pressure is plotted as a function of the upper radial displacement. To compute the entire shape of the load displacement curve, we again use an arc-length method and a Newton solution process. The maximum radial displacement of the upper edge corresponds to a circumferential strain of more than 800 %. In addition deformed configurations are shown in Figure 6.

### 6.4 Inflated Shallow Spherical Cap

A shallow spherical cap with material data given in Table 1 is considered in this example (see Wriggers and Taylor [12]). The radius of the cap is $R = 10$ and the thickness is $h_0 = .1$. We assume an initial displacement of the center point of $w_0 = R/100$ . The cap is loaded normal to the current configuration by a uniform pressure. By symmetry considerations a $5^0$ sector of the cap is modeled with 20 4-node elements. The computed curve of pressure versus displacement of the center point is shown in Figure 7, and plots of deformed meshes are contained in Figure 8.

### 6.5 Inflation of a Torus between two Plates

In the following example the inflation of a tire between two frictionless rigid plates is considered. Assuming membrane behavior in a simple model we discretize a thin walled torus, which is loaded by an internal constant pressure. The geometrical data of the torus are: inner radius $R_i = 40$, outer radius $R_a = 60$, and thickness $h_0 = 0.1$. The material is an incompressible Ogden model with constants for the stored energy function as given in Table 1. We consider rigid plates at $x_1 = \pm 60$. The contact constraint is enforced by means of a classical penalty method. Considering symmetry, only one quarter of the upper part of the torus is modeled using 100 4-node bilinear isoparametric

elements. The nodes at $R_i = 40$ are fixed. The computed curve of contact force versus internal pressure is shown in Figure 9 and a plot of the deformed mesh is contained in Figure 10. This plot shows that the structure undergoes large displacements and large strains.

### 6.6 Stretching of a Square Sheet with a Circular Hole

The last example is concerned with the stretching of a square sheet with a circular hole. This problem has been analyzed previously by Parisch [7]. The length of the square is $2L = 20$, the radius of the circle is $R = 3$, and the thickness is $h_0 = .1$. The edge at $x_1 = \pm 20$ is fixed in both directions. The material constants for a Mooney-Rivlin model are shown in Table 2.

**Table 2** Material Properties for Mooney-Rivlin Model

| r | $\mu_r$ | $\alpha_r$ |
|---|---|---|
| 1 | +50.000 | +2.000 |
| 2 | -14.000 | -2.000 |

Because of the symmetry of the structure we discretize one quarter of the sheet with 50 9-node elements. In Figure 11 the stretching force $F$ of the computed quarter is plotted against the strain $u/L$ and the deformed configuration is shown in Figure 12.

## 7. Conclusion

In this paper we present a theory for rubberlike membranes which undergo finite elastic strains. For hyperelastic material response a strain energy function formulated in terms of the principal values of the right stretch tensor is used. The incompressibility constraint is enforced exactly by use of the plane stress condition. The linearization of the stresses is derived analytically, which preserves the quadratic rate of convergence in a Newton solution process of the finite element equations. Since the initial geometry is approximated using an isoparametric approach, we are able to discretize arbitrarily shaped membranes. The numerical examples with nonconservative pressure loads are performed in a very effective process.

**Acknowledgements**

The support for the first author from the German foundation "Deutscher Akademischer Austauschdienst" within the NATO post-doctoral program is greatfully acknowledged.

References

1 Budianski, B.,"Notes on Nonlinear Shell Theory", J. Appl. Mech., 35, 393-401.

2 Gruttmann, F.,"Theorie und Numerik schubelastischer Schalen mit endlichen Drehungen unter Verwendung der Biot-Spannungen," Forschungs- und Seminarberichte aus dem Bereich der Mechanik der Universität Hannover, Bericht Nr. F88/1, Hannover, 1988.

3 Hughes, T. J. R., and Pister, K. S.,"Consistent Linearization in Mechanics of Solids and Structures," Computers & Structures, Vol. 8, 1978, pp. 391-397.

4 Needleman, A., "Inflation of Spherical Rubber Balloons", Int. J. Solids and Structures, 13, 1977, 409-421.

5 Ogden, R.W., "Elastic Deformations of Rubberlike Solids", in Mechanics of Solids, The Rodney Hill 60th Anniversary Volume, Editors: H.G. Hopkins and M.J. Sewell, Pergamon Press, 1981, 499-537

6 Ogden, R.W., Nonlinear Elastic Deformations, Ellis Horwood Limited, Chichester, U.K.

7 Parisch, H., "Efficient Non-linear Finite Element Shell Formulation Involving Large Strains", Eng. Comput., 1986, Vol. 3, 125-128.

8 Schweizerhof, K., Ramm E., "Displacement Dependent Pressure Loads in Nonlinear Finite Element Analysis", Computers & Structures, 18, 6, 1099-1114.

9 Simo, J. C., Fox D. D., and Rifai, M. S., "On a Stress Resultant Geometrically Exact Shell Model, Part III: Computational Aspects of the Nonlinear Theory", Comp. Meth. Appl. Mech. Engng., 79, 1990, 21-70.

10 Simo, J. C., and Taylor, R. L., " Quasi- Incompressible Finite Elasticity in Principal Stretches. Continuum Basis and Numerical Algorithms.", to appear in Comp. Meth. Appl. Mech. Engng.

11 Treloar, L.R.G., "Stress-strain Data for Vulcanized Rubber under Various Types of Deformation", Trans. Faraday Soc., 40, 1944, 59-70.

12 Wriggers, P., and Taylor R. L., " A Fully Nonlinear Axisymmetrical Membrane Element for Rubberlike Materials", preprint.

13 Zienkiewicz, O.C., and Taylor R.L., The Finite Element Method, 4th edition, Vol. 1, McGraw Hill, London, 1988.

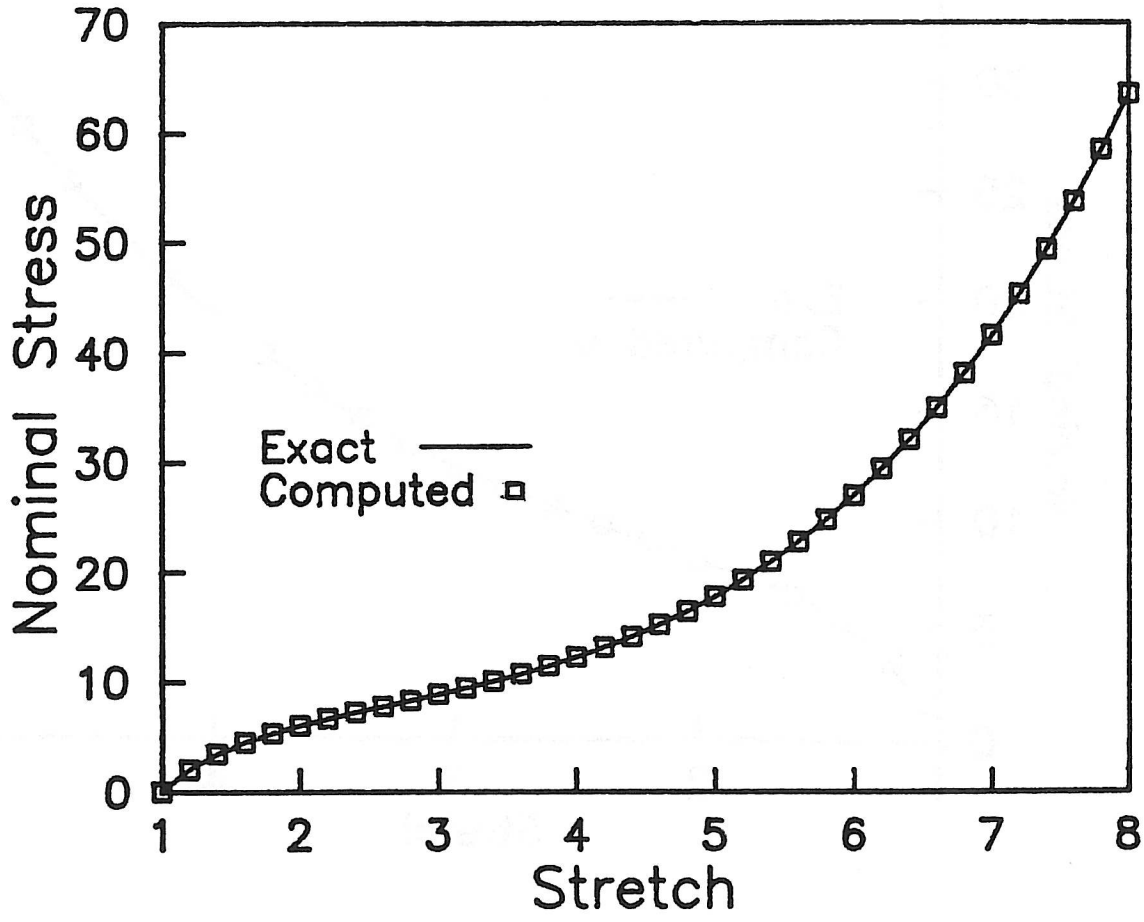


**Figure 1** Simple tension test of a three-term Ogden elastic material.

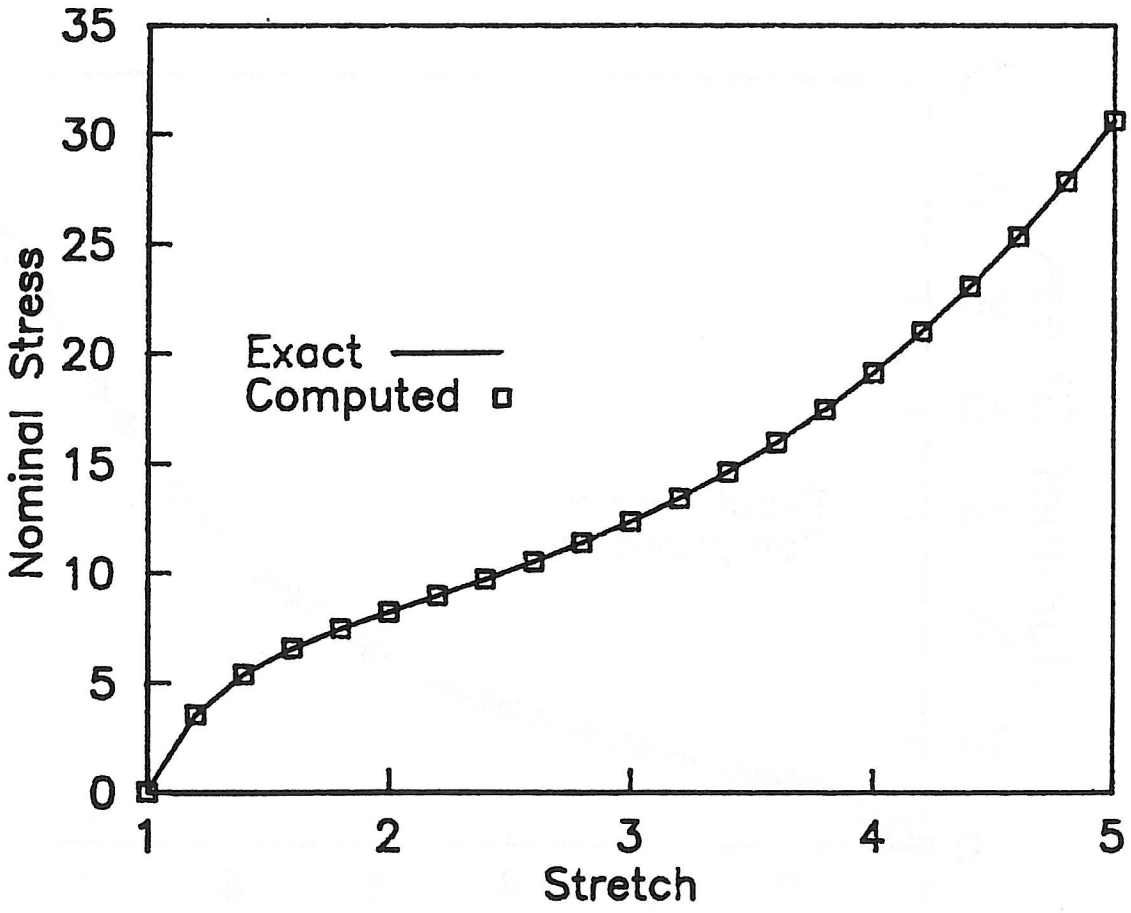


**Figure 2** Equibiaxial tension test of a three-term Ogden elastic material.

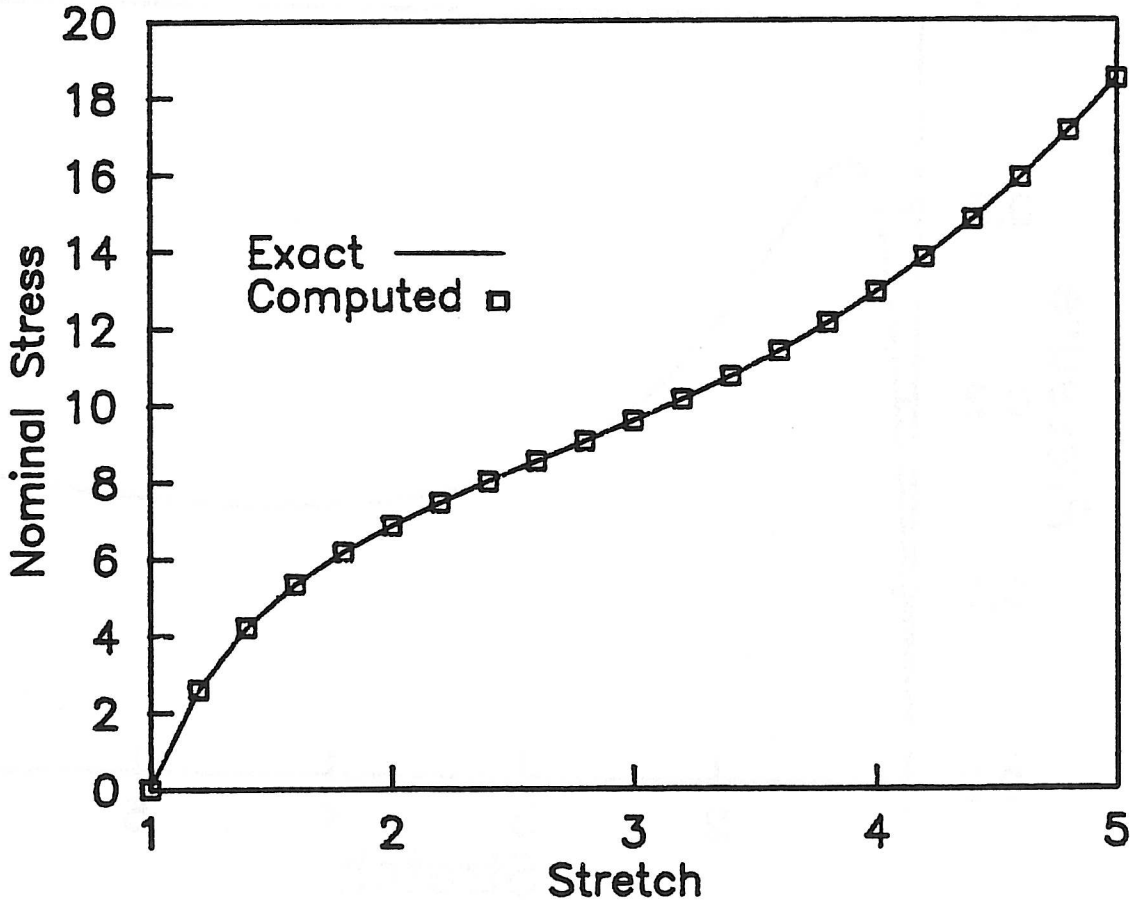


**Figure 3** Pure shear test of a three-term Ogden elastic material.

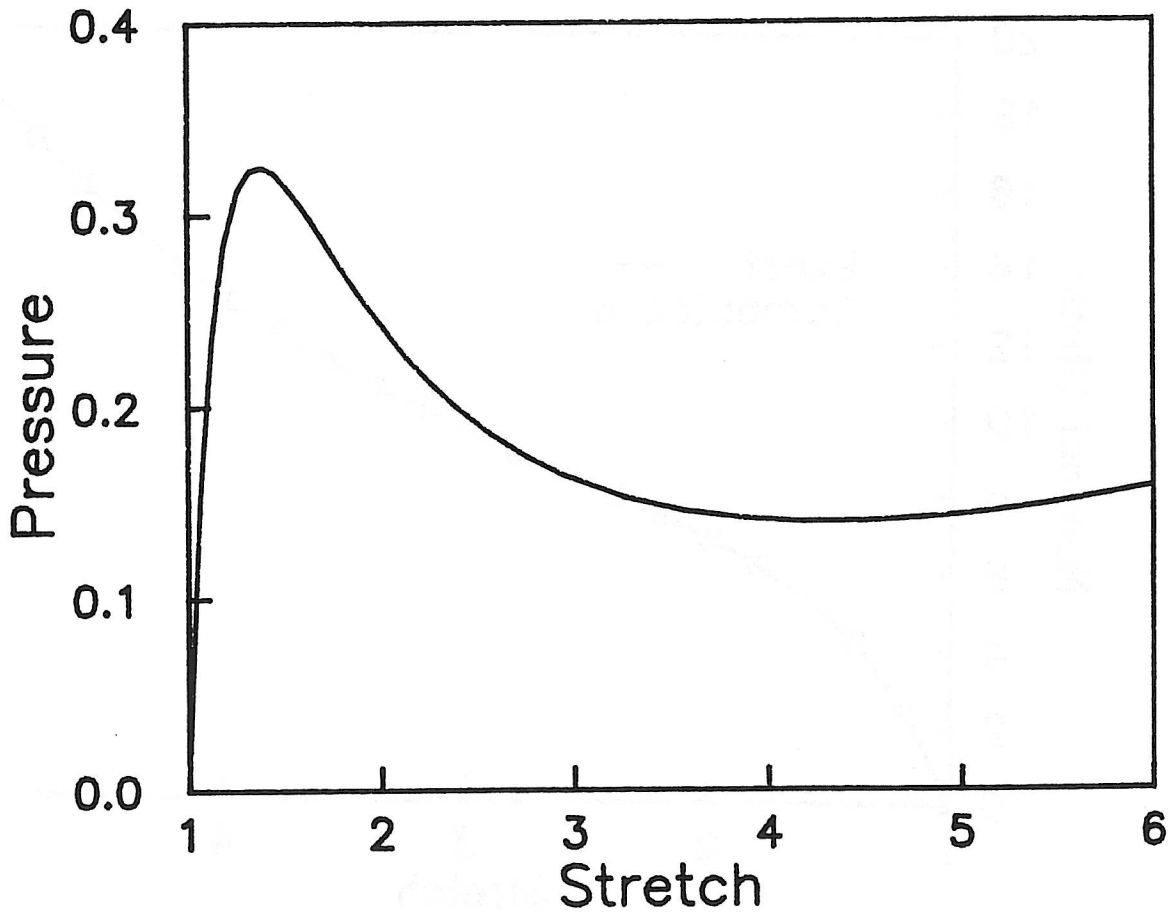


**Figure 4** Inflation of a spherical elastic balloon. Dimensionless pressure versus stretch.

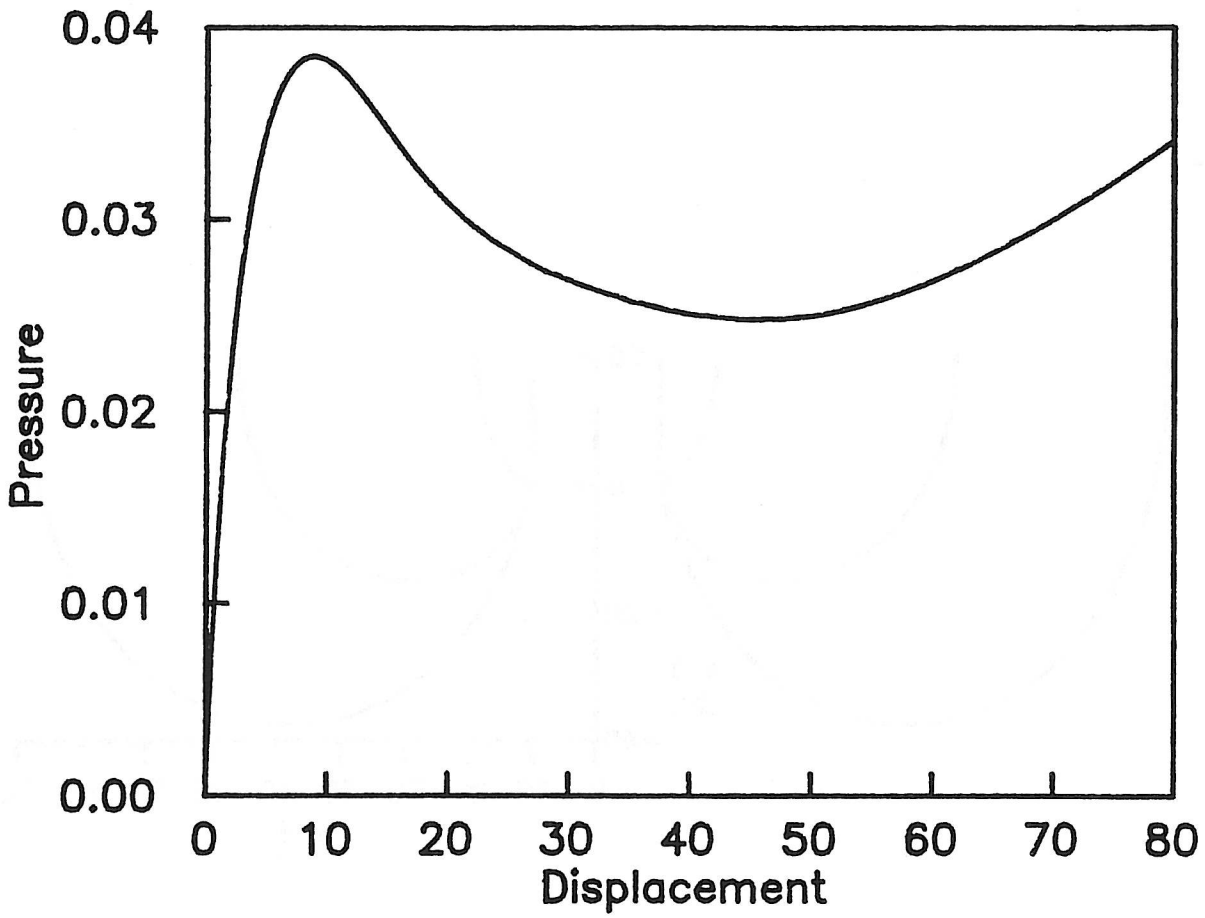


**Figure 5** Inflation of a circular cylinder. Internal pressure versus upper radial displacement.

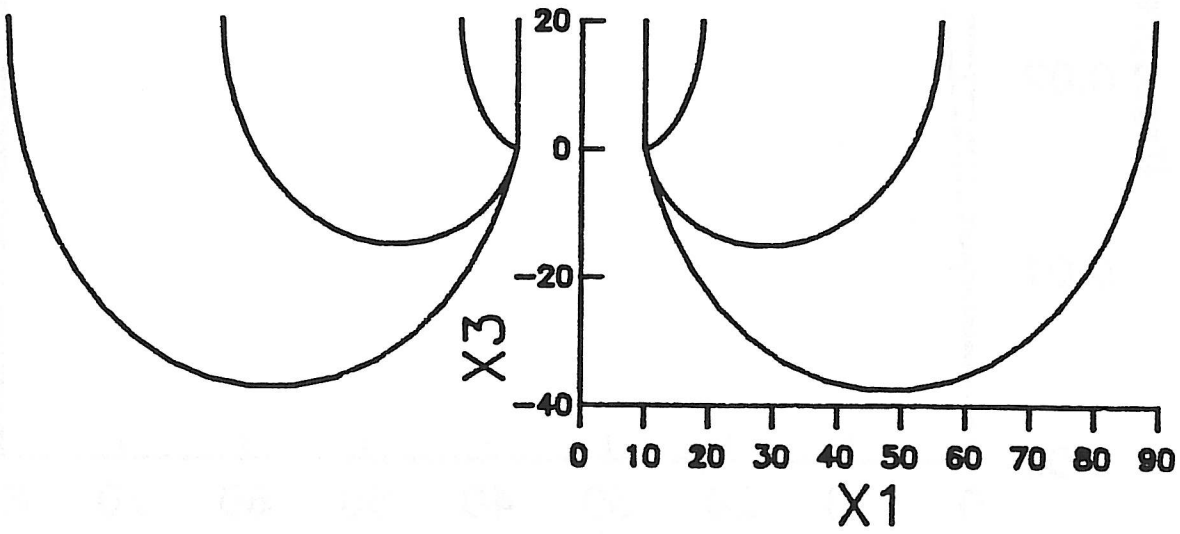


**Figure 6** Inflation of a circular cylinder. Deformed configurations.

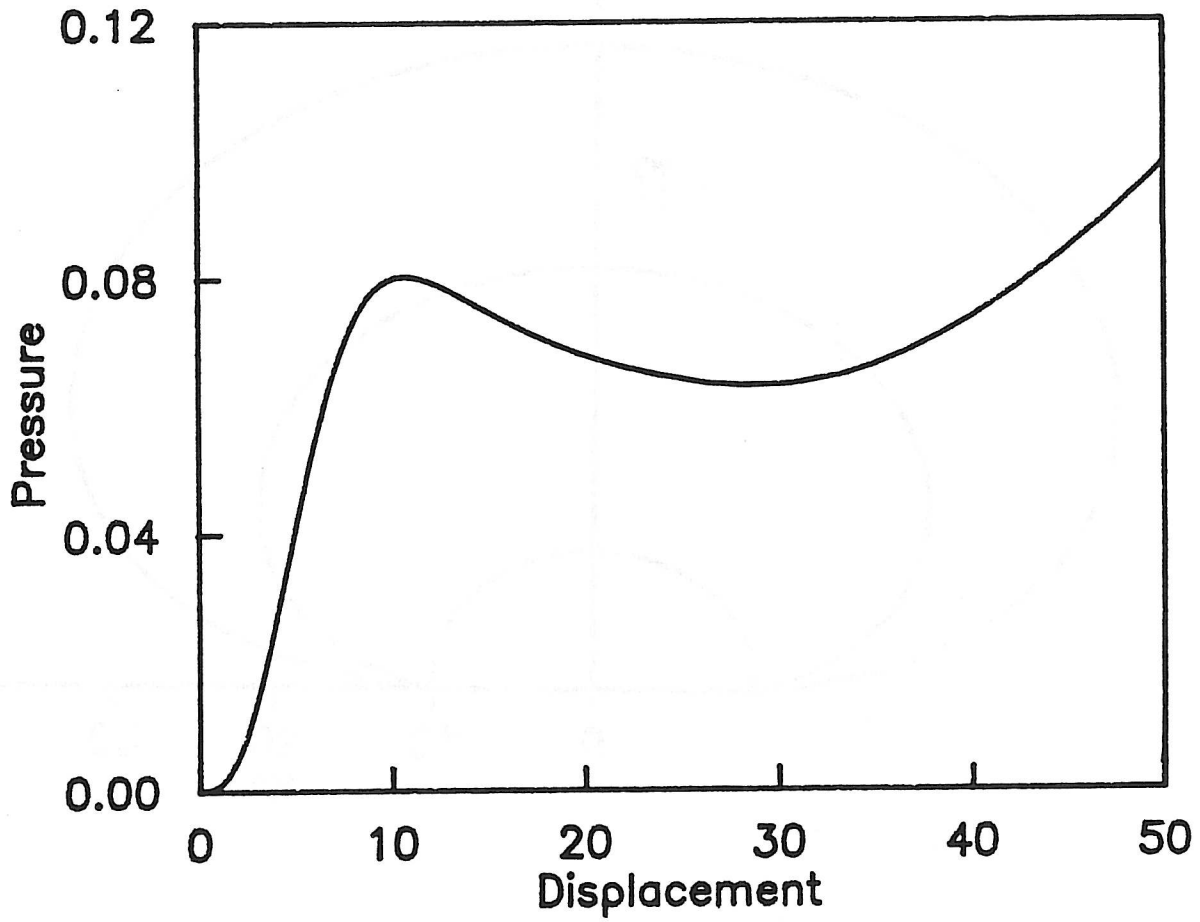


**Figure 7** Inflation of a shallow spherical cap. Pressure versus displacement of the centerpoint.

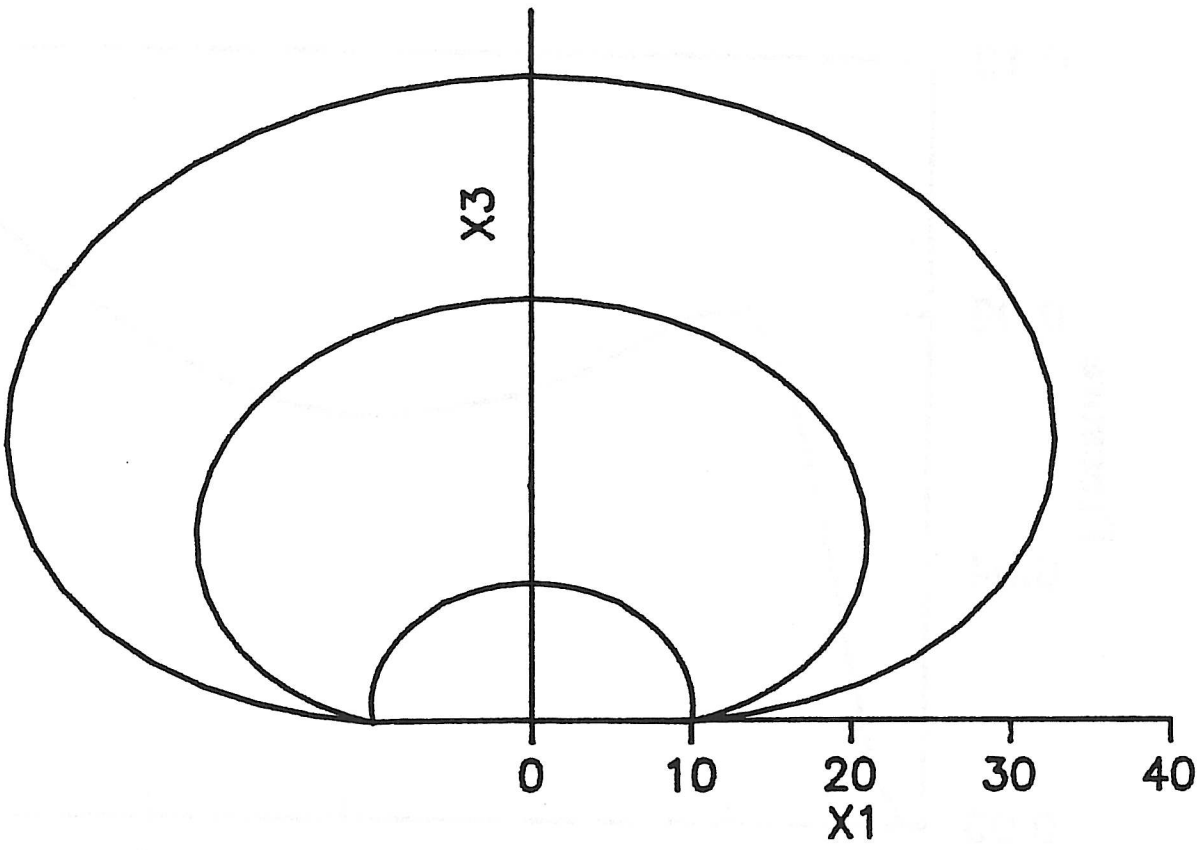


**Figure 8** Inflation of a shallow spherical cap. Deformed configurations.

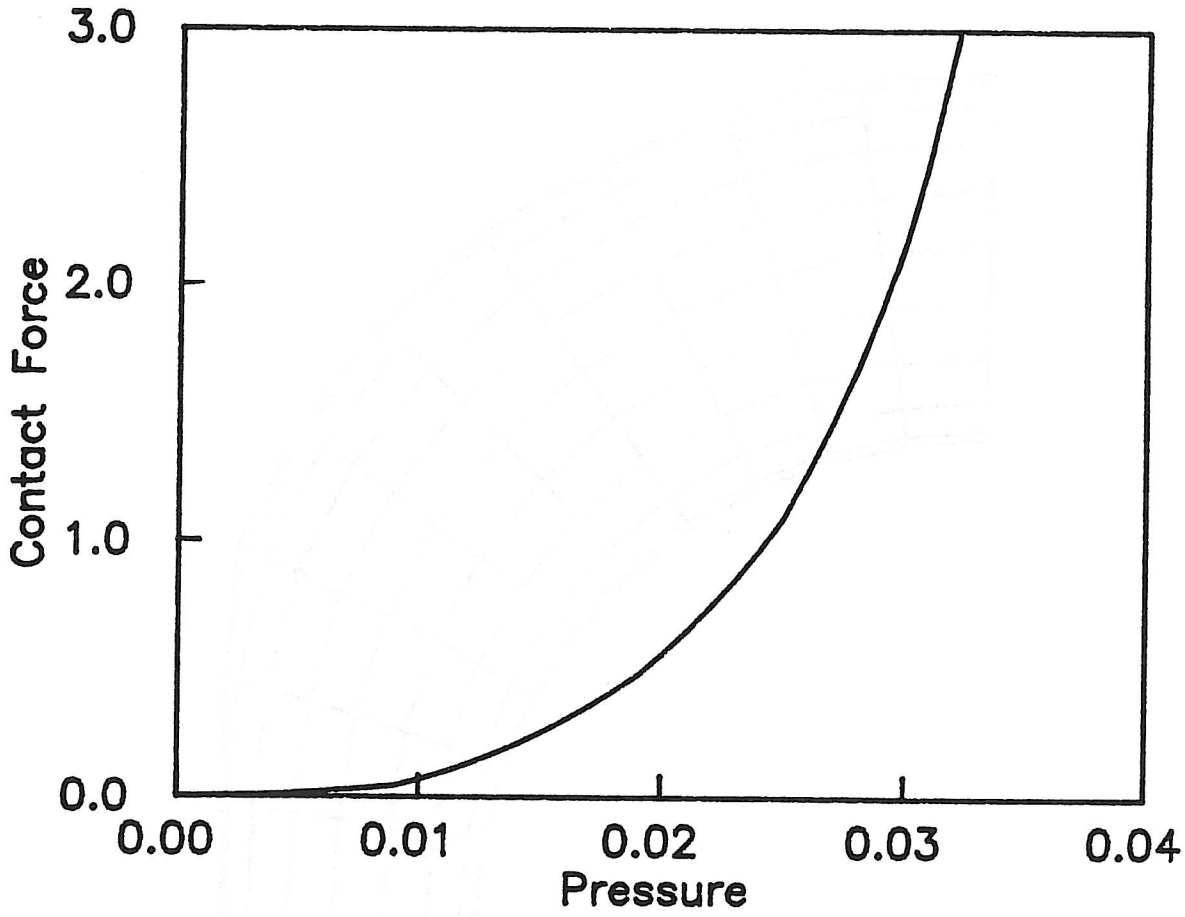


**Figure 9** Inflation of a torus between two rigid plates. Contact force versus internal pressure.

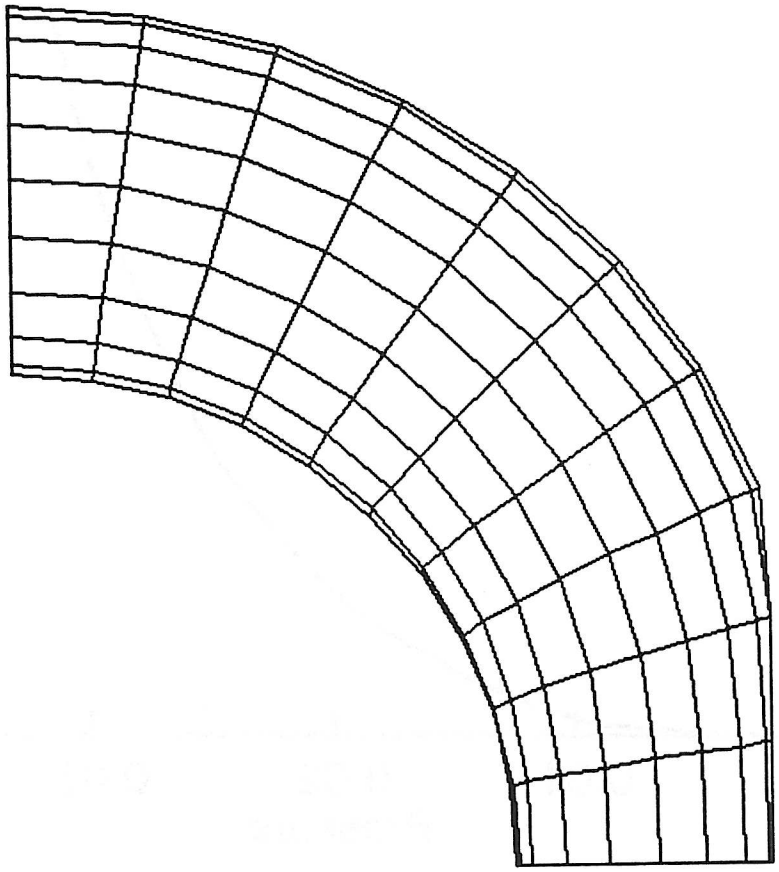

**Figure 10** Inflation of a torus between two rigid plates. Final deformed mesh.

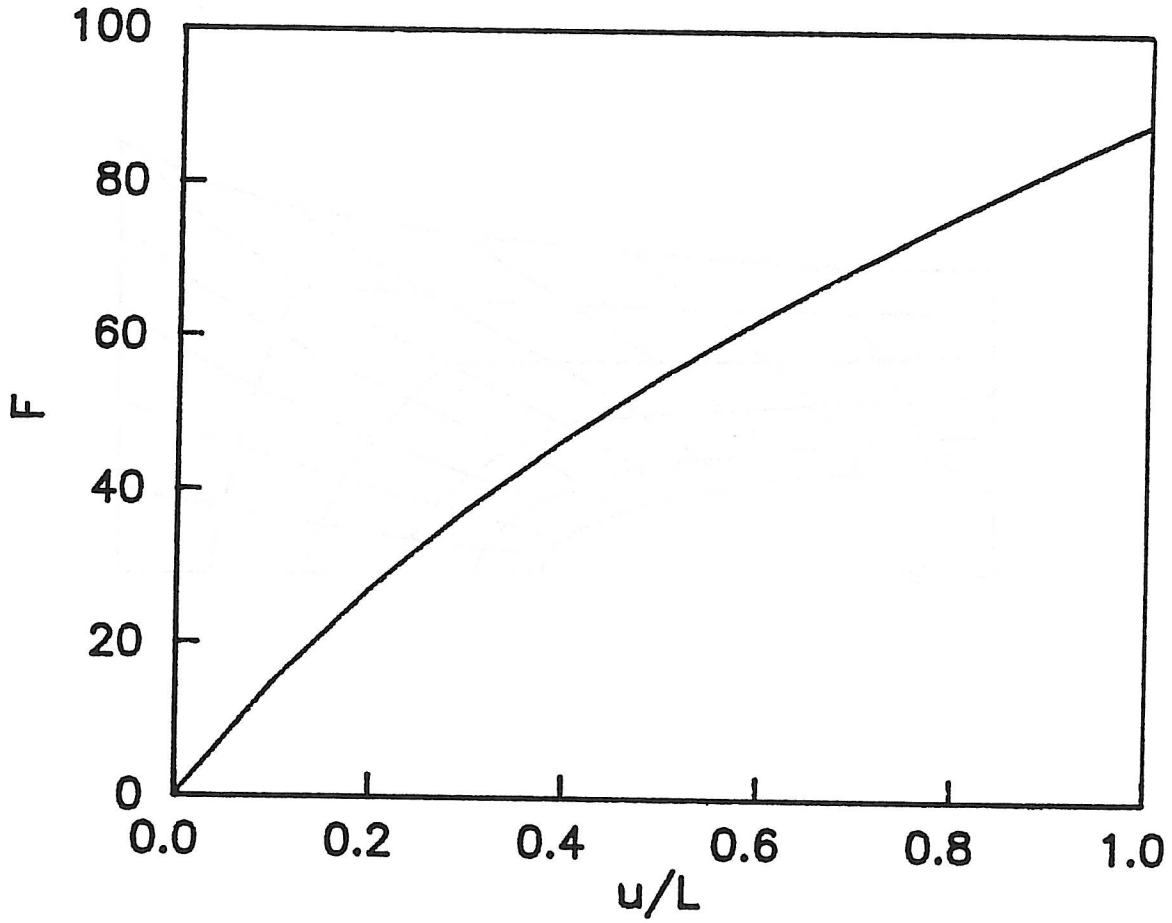


**Figure 11** Stretching of a square sheet with a circular hole. Load displacement curve.

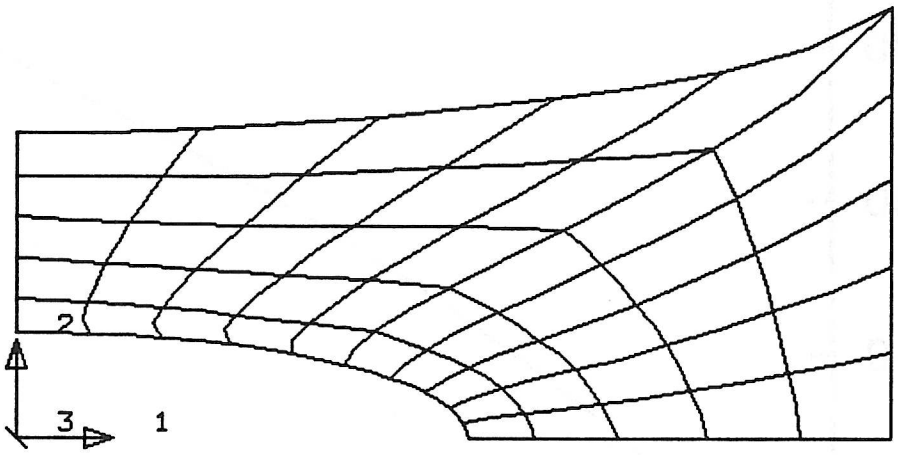


**Figure 12** Stretching of a square sheet with a circular hole. Final deformed mesh.